

OH ROTATIONAL LINES AS A DIAGNOSTIC OF THE WARM NEUTRAL GAS IN GALAXIES¹

JAVIER R. GOICOECHEA², JESUS MARTÍN-PINTADO AND JOSÉ CERNICHARO

Departamento de Astrofísica Molecular e Infrarroja, Instituto de Estructura de la Materia, CSIC, Serrano 121, 28006, Madrid, Spain
Accepted in ApJ Part I, 2004, October 6

ABSTRACT

We present *Infrared Space Observatory* (ISO) observations of several OH, CH and H₂O rotational lines toward the bright infrared galaxies NGC 253 and NGC 1068. As found in the Galactic clouds in Sgr B2 and Orion, the extragalactic far-IR OH lines change from absorption to emission depending on the physical conditions and distribution of gas and dust along the line of sight. As a result, most of the OH rotational lines that appear in absorption toward NGC 253 are observed in emission toward NGC 1068. We show that the far-IR spectrum of OH can be used as a powerful diagnostic to derive the physical conditions of extragalactic neutral gas. In particular, we find that a warm ($T_k \sim 150$ K, $n(\text{H}_2) \lesssim 5 \times 10^4 \text{ cm}^{-3}$) component of molecular gas with an OH abundance of $\simeq 10^{-7}$ from the inner $\lesssim 15''$ can qualitatively reproduce the OH lines toward NGC 253. Similar temperatures but higher densities ($\sim 5 \times 10^5 \text{ cm}^{-3}$) are required to explain the OH emission in NGC 1068.

Subject headings: galaxies: nuclei — galaxies: ISM — galaxies: individual (NGC253, NGC1068) — infrared: galaxies — ISM: molecules

1. INTRODUCTION

Galactic nuclei play a key role for our understanding of galactic evolution. The use of molecular diagnostics to extract their physical conditions helps to understand the nature of the prevailing scenarios, e.g., starbursts vs. active galactic nuclei (AGN). Space observations at mid- and far-IR wavelengths offer an unique opportunity to observe the pure rotational lines of light hydrides, the simplest chemical building blocks. In particular, H₂ observations have revealed the presence of a considerable amount of “warm” (excitation temperatures, T_{ex} , around 100-200 K) neutral gas in the Galactic Center (GC; Rodríguez-Fernández et al. 2001) and also in galaxies (Rigopoulou et al. 2002).

ISO has given the opportunity to observe polar species that are sensitive to a broad range of densities and kinetic temperatures. The far-IR spectrum, and thus the molecular content, of molecular clouds such as Sgr B2 in the GC (Goicoechea et al. 2004) is surprisingly similar to that observed in ultra-luminous IR galaxies such as Arp 220 (González-Alfonso et al. 2004). One of the species with the largest abundance is the OH radical.

Bright IR galaxies containing OH usually show megamaser emission at 18 cm. These lines arise from the hyperfine splitting of the OH $^2\Pi_{3/2}$ $J=3/2$ ground rotational state. Among the possible excitation mechanisms of these masers; near- and far-IR pumping, collisions and UV radiation, the far-IR excitation seems to be the dominant mechanism inverting the population of the hyperfine levels (e.g. Skinner et al. 1997). Furthermore, the relative population of the OH levels is governed by the far-IR pure rotational lines and detailed treatment

of the rotational excitation is required to analyze the OH radio lines at 18 cm but also the $^2\Pi_{3/2}$ $J=5/2$ and $^2\Pi_{1/2}$ $J=1/2$ lines at 5 and 6 cm (Randell et al. 1995).

The OH ground-state rotational line at $\sim 119 \mu\text{m}$ was first detected in absorption toward Sgr B2 (Storey et al. 1981), while several excited rotational lines have been analyzed by Goicoechea & Cernicharo (2002). A detailed analysis of the far-IR spectrum of OH has been also carried out in the Orion region (Watson et al. 1985; Vicuso et al. 1985; Melnick et al. 1987, 1990; Betz & Boreiko 1989). The observed lines appear in emission and some of them even show more complex P-Cygni profiles. Different excitation conditions determine the distinct OH spectral signatures observed toward Orion and Sgr B2.

These studies have shown that OH can be a powerful probe of the warm neutral gas in molecular clouds. Scaled to extragalactic studies, OH can thus provide significant information about star forming regions and the heating processes in the inner arcsecs of a galaxy, in addition to the understanding of the megamaser excitation mechanism. Moreover, OH is a key molecule in the gas-phase chemistry networks. The presence of OH in the warmer regions may enhance and even dominate the formation of other O-bearing species, so that the determination of its abundance is also relevant to understand the prevailing chemistry.

In this letter we present and analyze several OH far-IR lines, involving levels up to ~ 420 K, toward the Starburst galaxy NGC 253 and the Seyfert 2 galaxy NGC 1068. We compare these extragalactic OH lines with our far-IR observations of Sgr B2(M) and Orion IRC2, and run simple non-LTE radiative transfer models to qualitatively understand the behavior of the detected lines.

2. OBSERVATIONS AND DATA REDUCTION

Several pure rotational lines of OH appear in the wavelength coverage of the Long- and Short- Wavelength Spectrometers (LWS: Clegg et al. 1996; SWS: de Graauw et al. 1996) on board ISO (Kessler et al. 1996). Bradford et al. (1999) have previously presented LWS Fabry-

Electronic address: javier@damir.iem.csic.es

¹ Based on observations with ISO, an ESA project with instruments funded by ESA Member States (especially the PI countries: France, Germany, the Netherlands and the United Kingdom) and with participation of ISAS and NASA.

² On leave to the Laboratoire d'Étude du Rayonnement et de la Matière, UMR 8112, CNRS, École Normale Supérieure et Observatoire de Paris, 24 rue Lhomond, 75231 Paris Cedex 05, France

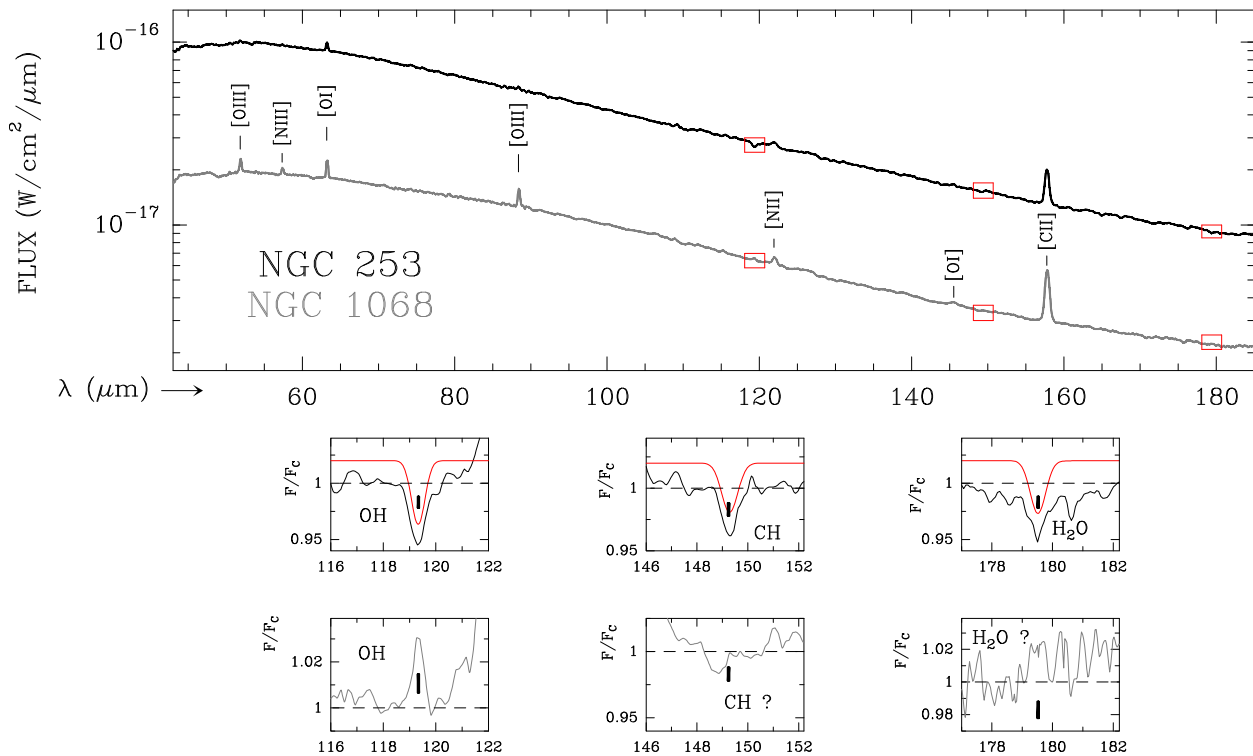


FIG. 1.— ISO/LWS grating observations of NGC 253 and NGC 1068. The ordinate corresponds to the flux and the abscissa is the rest wavelength in μm . Atomic fine structure lines are labeled. Zooms around selected wavelengths are also shown in the smaller panels with models of the ground-state rotational lines of OH, CH and H_2O (see text). The ordinate of these panels is the continuum normalized flux.

Perot (FP) observations of the OH ground-state line at $\sim 119 \mu\text{m}$ toward NGC 253 ($v_{\text{LSR}} \simeq 250 \text{ km s}^{-1}$), while Spinoglio et al. (1999) presented the full LWS grating spectrum of NGC 1068 ($v_{\text{LSR}} \simeq 1140 \text{ km s}^{-1}$). In this work, we have used the public ISO Data Archive (IDA) and analyzed the target dedicated time numbers (TDTs) 24701103, 56901708 (for NGC 253) and 60500401 and 60501183 (for NGC 1068). The spectral resolution of the LWS/grating is $\lambda/\Delta\lambda \sim 200$. The OH ${}^2\Pi_{1/2}$ - ${}^2\Pi_{3/2}$ $J=5/2$ - $3/2$ cross-ladder line at $\sim 34 \mu\text{m}$ was observed with the SWS/grating with a spectral resolution of $\lambda/\Delta\lambda \sim 1500$ (TDTs 37902123 and 64302927). The LWS beam has a $\sim 80''$ diameter while the SWS aperture in the $\sim 34 \mu\text{m}$ range is $17'' \times 40''$. LWS and SWS data were analyzed using the ISO Spectral Analysis Package³ (ISAP). Typical routines include: deglitching spikes due to cosmic rays, oversampling and averaging individual scans, removing baseline polynomials and extracting line fluxes by fitting Gaussians. More details can be found in the LWS handbook (Gry et al. 2003). The full ISO/LWS spectra of NGC 253 and NGC 1068 are shown in Figure 1 while several OH rotational lines are shown in Figure 2.

3. RESULTS

The far-IR spectrum of NGC 253 and NGC 1068 (Fig. 1, *large panel*) is dominated by the thermal emission of dust and by atomic fine structure emission lines (Negishi et al. 2001). The signal-to-noise ratio of these

spectra is lower than the *ISO/LWS* spectrum of Arp 220, which is very rich in molecular features (see González-Alfonso et al. 2004). However, the ground-state rotational lines of OH, CH and H_2O are clearly observed in NGC 253 and possibly in NGC 1068 (Fig. 1, *small panels*). Figure 2 shows in more detail the OH ~ 34 , ~ 53 and $\sim 79 \mu\text{m}$ cross-ladder lines, the ~ 84 and $\sim 119 \mu\text{m}$ lines of the ${}^2\Pi_{3/2}$ ladder, and the $\sim 163 \mu\text{m}$ line of the ${}^2\Pi_{1/2}$ ladder toward NGC 253 and NGC 1068. For comparison we also show the OH spectra of archetype star forming regions in our Galaxy: Sgr B2 and Orion IRC2. It is interesting to note that the behavior of the OH lines in NGC 1068 follows that of Orion IRC2, i.e., emission in all the observed lines (except in the ~ 53 and $\sim 34 \mu\text{m}$ lines). On the other hand, the OH lines in NGC 253 have a similar behavior than in Sgr B2(M), i.e., absorption in the ${}^2\Pi_{3/2}$ ladder and cross-ladder lines and emission in the ${}^2\Pi_{1/2}$ ladder (Goicoechea & Cernicharo 2002). Hence, the OH rotational lines show distinct trends in two prototype galaxies where the nuclei activity is also different.

Due to its large dipole moment and rotational constant, radiative pumping of the rotational levels must be taken into account as long as collisions to compute the OH level population. For the typical temperatures of molecular clouds, LTE can only be achieved at very high H_2 densities, $n(\text{H}_2) > 10^{10} \text{ cm}^{-3}$. Hence, the knowledge of the dust continuum properties and its distribution respect to the molecular gas is needed to analyze the OH excitation.

4. DISCUSSION

In order to qualitatively understand the contribution of the physical and geometrical parameters to the OH

³ ISAP is a joint development by the LWS and SWS Instruments Teams and Data Centers. Contributing institutes are CESR, IAS, IPAC, MPE, RAL, and SRON.

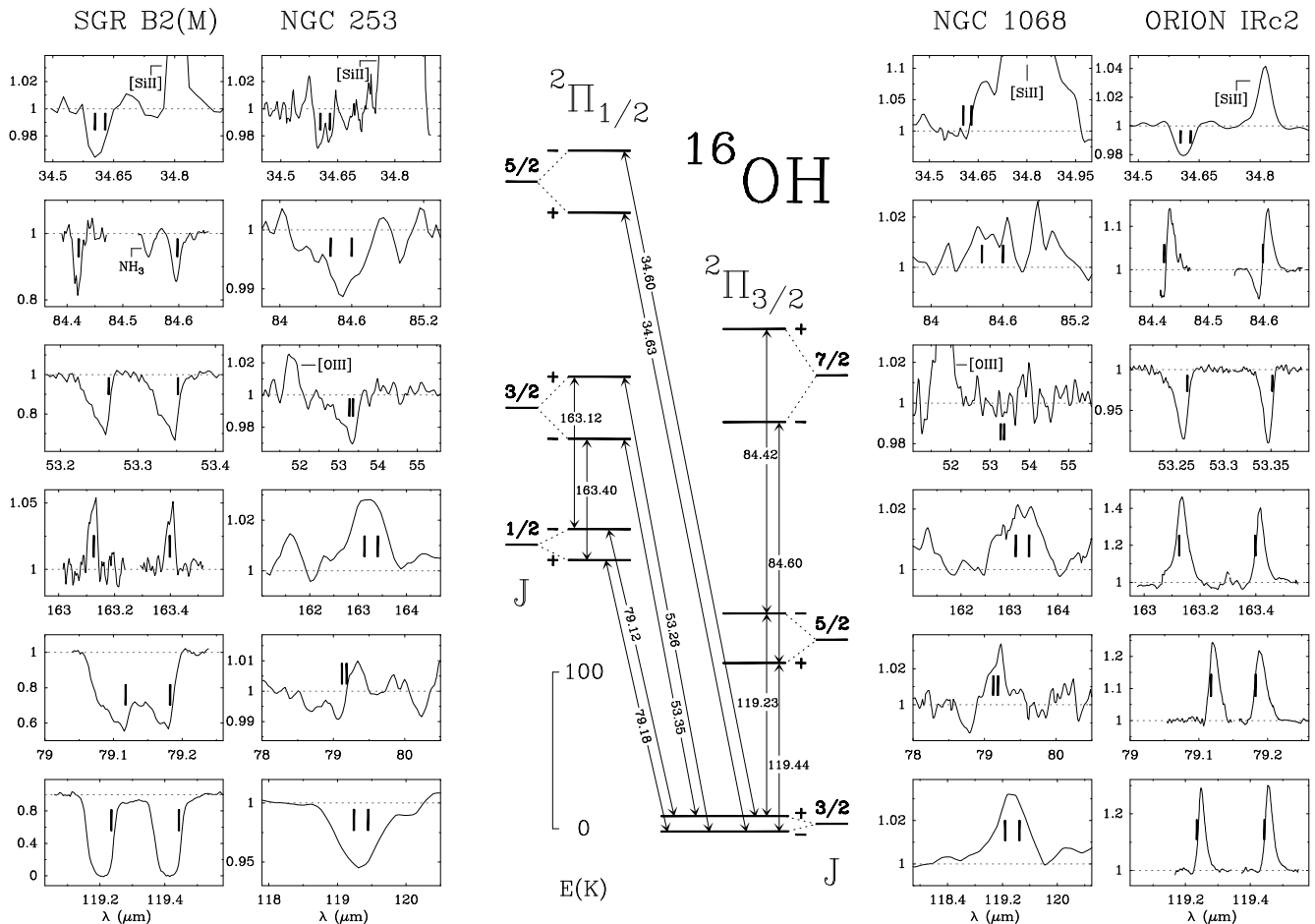


FIG. 2.— ISO observations of OH rotational lines towards Sgr B2(M) (from Goicoechea & Cernicharo 2002), NGC 253, NGC 1068 and Orion IRC2. The ordinate scale corresponds to the continuum normalized flux. The abscissa in all the boxes is the rest wavelength in microns. The vertical thick lines indicate the rest wavelengths of the different OH Λ -doublets. The Λ -doublets are spectrally resolved in the *Fabry–Perot* observations otherwise *grating* observations are presented. The rotational energy diagram of OH (neglecting hyperfine structure) and the observed transitions are also shown in the middle of the figure. The Λ -doubling has been exaggerated for clarity.

spectrum, we have modeled the first 20 rotational levels of OH with two radiative transfer codes (LVG and non-local; Cernicharo et al. 2000). The hyperfine structure of OH was not included in the calculations. Collisional cross sections of OH with H_2 from Offer et al. (1994) have been used with an H_2 ortho-to-para ratio of 3.

It is obviously more difficult to model the molecular emission/absorption from a galactic nucleus (an ensemble of molecular clouds) than to model a single molecular cloud. Since the observed extragalactic OH lines are not velocity resolved and the angular resolution is larger than the dimensions of the observed sources, we have just considered a simplified model of an *IR core* + *OH shell* as a first approximation. Therefore, we have adopted a spherical geometry consisting of a shell of radius R_{shell} and continuum core of radius R_{core} . The exact radius determine the resulting OH column density and the properties of the dust emission, however, *ISO* observations can not provide that information. Then, we have compared the synthetic continuum-normalized spectrum with the *ISO* observations considering that the source is composed of several clouds with the same physical conditions but do not overlap in the line-of-sight (see the discussion by González-Alfonso et al. 2004).

In the case of NGC 253, the mid-IR continuum is confined to the inner $\sim 10''$ of the galaxy (Telesco et al. 1993). We have taken this as a lower limit to R_{core} in the far-IR. In the other hand, low- J CO observations reveal that the molecular gas extends up to $\sim 50''$ (Harrison et al. 1999). However, CO $J=7-6$ ($E_u \sim 150$ K) observations show that the bulk of this emission is confined to the inner $\sim 15''$ (Bradford et al. 2003). In addition, several OH masers at ~ 18 cm have been detected within the central $\sim 10''$ of the nucleus (Frayser et al. 1998). We have assumed that the far-IR OH lines and the IR continuum arises from the $\sim 15''$ region, but we note that a more detailed model of NGC 253 could include an extended component of low excitation OH gas (that will enhance the absorption of the ~ 119 μm fundamental line; see González-Alfonso et al. 2004 for the case of Arp 220). In fact, observations of the extended absorption of OH 18 cm lines reveal that OH in the ground-state is present as far as $\sim 45''$ from the nucleus (Turner 1985). However, here we are mainly interested in the general behavior of the higher energy OH lines and since the ISO/LWS angular/spectral resolution is poor, we will not add more complexity to the calculations in this work. We have taken $R_{core}/R_{shell}=0.9$, although we also inves-

tigate the effect of the dilution of the radiation arising from the core. From a gray-body fitting of the LWS continuum emission we have adopted a dust opacity law $\tau_\lambda = \tau_{119} [119/\lambda(\mu\text{m})]^{1.5}$ with $\tau_{119}=1$ and $T_d=41$ K.

To compare with the NGC 1068 observations, we have considered that the OH emission also arises from a single component with similar geometry and continuum emission as for NGC 253. However, our calculations showed that the OH emission fluxes could only be reproduced if the emission arises from a more compact component with $\theta_{shell} \lesssim 10''$ and $\theta_{core} \sim 5''$. This suggests that the OH emission may be dominated by dense gas in cloud cores near the nucleus. This is the case of HCN observed at higher resolution (Jackson et al. 1993; Tacconi et al. 1994). Note that OH masers at ~ 18 cm have been found in the inner arcsec of NGC 1068 (Gallimore et al. 1996). Higher angular resolution is needed to estimate the contribution of the Starburst ring to the OH emission.

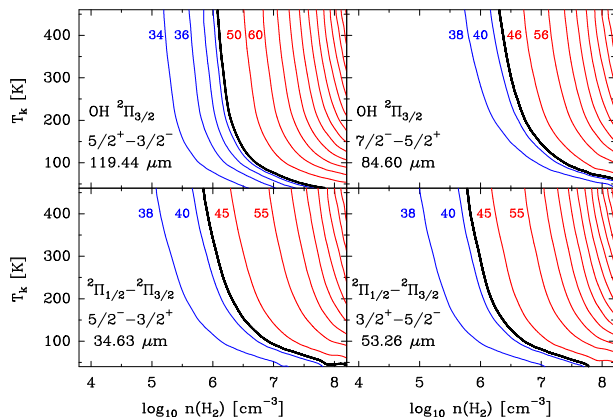


FIG. 3.— Large Velocity Gradient models of different kinetic temperature and density for the observed OH lines in NGC 253. The OH column density is $6.5 \times 10^{16} \text{ cm}^{-2}$. The thick contour corresponds to the equivalent temperature of the continuum source ($R_{core}/R_{shell}=0.9$ and $\tau_{119}(\text{dust})=1$). To the left of this contour, lines are predicted in absorption.

Several results from the LVG computations are shown in Fig. 3. The excitation temperature of each rotational transition as a function of gas temperature (T_k) and density is shown in each panel. The thick black contour represents the equivalent temperature of the continuum. Therefore, to the left of this contour, the OH lines are predicted in absorption. From the excitation models it is clear that high densities are required to observe the OH lines in emission, i.e., the case of NGC 1068. If the R_{core}/R_{shell} ratio is decreased or the shell thickness is increased, the iso- T_{ex} contours on Fig. 3 (the absorption/emission boundary), will move to the left toward lower densities. This is due to the increase of the reemission from the gas that do not absorb the core emission. Note that reemission also scales with the thickness of the shell.

To investigate the effect of the radiative coupling between components of different physical conditions we have also run several nonlocal models (see González-Alfonso & Cernicharo 1993) for OH including both the gas and dust transfer (Cernicharo et al. 2000). We run calculations for different geometrical and physical conditions. As an example, Fig. 4 shows some of the results

for the ~ 163.12 and $\sim 79.18 \mu\text{m}$ lines. The $^2\Pi_{1/2} J=3/2-1/2$ line at $\sim 163 \mu\text{m}$ is observed in emission in all the sources. Goicoechea & Cernicharo (2002) showed that the $\sim 163 \mu\text{m}$ emission in Sgr B2(M), were the far-IR continuum is optically thick, is produced by a fluorescent-like mechanism in low density ($< 10^4 \text{ cm}^{-3}$) warm gas ($T_k \simeq 150\text{-}300$ K). In the other hand, Melnick et al. (1987) showed that $T_k < 100$ K and $n(\text{H}_2) > 10^{6-7} \text{ cm}^{-3}$ are required to fit the observed emission in Orion IRC2 shocked region, so that collisions dominate the excitation. However, these authors argued that even with those conditions, the radiative pumping to the levels that give rise to the $\sim 163 \mu\text{m}$ emission has to be taken into account.

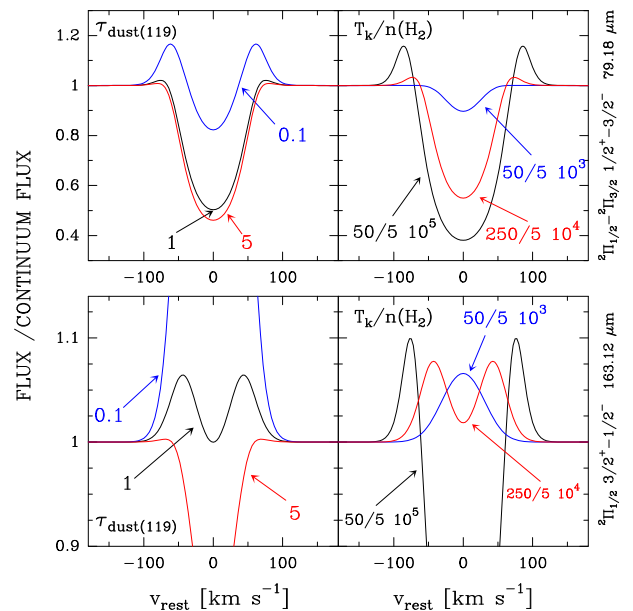


FIG. 4.— Nonlocal models for the $^2\Pi_{1/2}-^2\Pi_{3/2} J=1/2^+-3/2^-$ transition at $79.18 \mu\text{m}$ (upper panel) and for the $^2\Pi_{1/2} J=3/2^+-2/2^-$ transition at $163.12 \mu\text{m}$ (lower panel). Line intensities have been normalized to the continuum emission. The abscissa is the rest velocity. The velocity resolution in the line profiles is 1 km s^{-1} . All the models have $\chi(\text{OH})=10^{-7}$. Left panels: Models with $R_{core}/R_{shell}=0.9$, $T_k=150$ K, $n(\text{H}_2)=5 \times 10^4 \text{ cm}^{-3}$ and variable dust opacity of the continuum source. Right panels: Models with $R_{core}/R_{shell}=0.9$, $\tau_{119}(\text{dust})=1$ and variable T_k and $n(\text{H}_2)$.

From our calculations it is clear that while at low OH abundances [$\chi(\text{OH})$] the ~ 79 , ~ 53 and $\sim 34 \mu\text{m}$ cross-ladder absorption depths are proportional to the OH column density [$N(\text{OH})$], the $\sim 163 \mu\text{m}$ emission over the continuum flux is nearly constant because the emission mechanism at low densities depends mainly on the continuum radiation. At high $\chi(\text{OH})$, reemission start to dominate the ~ 79 and $\sim 119 \mu\text{m}$ lines. Taking into account the simplicity of our calculations, we find $\chi(\text{OH}) \sim 10^{-7}$ as the most realistic value for NGC 253. Lower values are required if the core emission is more diluted, otherwise reemission dominates. On the other hand, larger abundances can be possible if OH emission/absorption and far-IR continuum emission have different dilution factors.

Density and T_k determine the role of collisional excitation. For low $n(\text{H}_2)$, radiative excitation dominates, and the OH spectrum is less sensitive to $n(\text{H}_2)$ and T_k variations. This seems to be the case of NGC 253 inner re-

gions and the GC molecular clouds, which probably share similar physical conditions. The effect of T_k is more relevant for higher dilution of the core radiation. We found that the model with $T_k \sim 150$ K and $n(\text{H}_2) \lesssim 5 \times 10^4 \text{ cm}^{-3}$ better fits the OH observations of NGC 253. This temperature is in between the T_{ex} derived from the $\text{H}_2 S(0)$ line by Rigopoulou et al. (2002) and the T_k derived from the CO $J=7-6$ line emission by Bradford et al. (2003). Finally, from the ground-state rotational lines of CH and H_2O toward NGC 253 and assuming intrinsic line widths of $\sim 200 \text{ km s}^{-1}$ and $T_{ex} < T_d$ (absorption lines) we found a lower limit for the CH and H_2O column densities of $\sim 5 \times 10^{13}$ and $\sim 1 \times 10^{15} \text{ cm}^{-2}$ respectively (Fig. 1).

Similar arguments also apply for NGC 1068. Following Sternberg et al. (1994) we have first assumed $T_k = 50$ K. Taking into account the simplifications in our models, the calculations for NGC 1068 show that the density must be larger than 10^6 cm^{-3} , otherwise the OH lines are still predicted in absorption. For $n(\text{H}_2) = 5 \times 10^5 \text{ cm}^{-3}$, the temperature has to be increased to ~ 150 K to fit the observations, so that it is likely that a fraction of warm neutral gas also exists in the clouds near the nucleus of NGC 1068. Intense emission in other OH rotational lines (not detected by ISO) are predicted for higher densities and temperatures.

5. CONCLUSIONS

Irrespective of the specific nuclei scenario and of the density of the dominant molecular clouds, OH observations show that a similar component of warm neutral gas ($T_k \sim 150$ K) exists in NGC 253 and NGC 1068. This component can influence the chemistry as neutral-neutral reactions involving OH start to be efficient for the production of other oxygen molecules such as H_2O and SiO. The contribution of PDRs, shocks, X-rays and cosmic rays to the heating of such component in Seyfert vs. Starburst galaxies is still far from settled. Future works using diagnostics of the warm gas will be extremely useful. In particular, several rotational lines of light hydrides such as OH, CH and H_2O will be observed at larger angular resolution by the HIFI and PACS instruments, on board Herschel in many galactic and extragalactic sources.

We thank Spanish DGES and PNIE for funding support under grants PANAYA2000-1784, ESP2001-4516, AYA2002-10113, ESP2002-01627 and AYA2003-02785.

REFERENCES

- Betz, A.L., & Boreiko, R.T. 1989, ApJ, 346, L101
Bradford, C.M., et al. 1999, The Universe as Seen by ISO. Eds. P. Cox & M. F. Kessler. ESA-SP 427., p. 861
Bradford, C.M., et al. 2003, ApJ, 586, 891
Cernicharo, J., Goicoechea, J.R. & Caux, E. 2000, ApJ, 534, L199
Clegg, P.E., et al. 1996, A&A, 315, L38
de Graauw, T. et al. 1996, 315, L49
Frayser, D. T., Seaquist, E. R., & Frail, D. A. 1998, AJ, 115, 559
Gallimore, J. F., Baum, S. A., O'Dea, C. P., Brinks, E., & Pedlar, A. 1996, ApJ, 462, 740
Goicoechea, J.R., & Cernicharo, J. 2002, ApJ, 576, L77
Goicoechea, J.R., Rodríguez-Fernandez, N.J. & Cernicharo, J. 2004, ApJ, 600, 214
González-Alfonso, E. & Cernicharo, J. 1993, A&A, 279, 503
González-Alfonso, E., Smith, H.A., Fisher, J. & Cernicharo, J. 2004, ApJ, 613, 247
Gry, C. et al. 2003, The ISO Handbook', Volume III - LWS - The Long Wavelength Spectrometer Version 2.1. ESA SP-1262, 2003.
Harrison, A., Henkel, C., & Russell, A. 1999, MNRAS, 303, 157
Jackson, J.M., Paglione, T.A. D., Ishizuki, S., & Nguyen-Q-Rieu 1993, ApJ, 418, L13
Kessler, M.F., et al. 1996, A&A, 315, L27
Melnick, G.J., Genzel, R., & Lugten, J.B. 1987, ApJ, 321, 530
Melnick, G.J., Stacey, G.J., Genzel, R., Lugten, J.B. & Poglitsch, A. 1990, ApJ, 348, 161
Negishi, T., Onaka, T., Chan, K.-W., & Roellig, T. L. 2001, A&A, 375, 566
Offer, A.R., van Hemert, M.C., & van Dishoeck, E.F. 1994, JChPh, 100, 362
Randell, J., Field, D., Jones, K. N., Yates, J. A. & Gray, M. D. 1995, A&A, 300, 659
Rigopoulou, D., Kunze, D., Lutz, D., Genzel, R. & Moorwood, A. F. M. 2002, 389, 374
Rodríguez-Fernandez, N.J. et al. 2001, A&A, 365, 174
Skinner, C. J., Smith, H. A., Sturm, E., Barlow, M. J., Cohen, R. J. & Stacey, G. J. 1997, Nature, 386, 472
Spinoglio, L. et al. 1999. The Universe as Seen by ISO. Eds. P. Cox & M. F. Kessler. ESA-SP 427., p. 969
Sternberg, A., Genzel, R., & Tacconi, L. 1994, ApJ, 436, L131
Tacconi, L. J., Genzel, R., Blietz, M., Cameron, M., Harris, A. I., & Madden, S. 1994, ApJ, 426, L77
Storey, J., Watson, D.M., & Townes, C.H. 1981, ApJ, 244, L27
Telesco, C. M., Dressel, L. L., & Wolstencroft, R. D., 1993, ApJ, 414, 120.
Turner, B. E. 1985, ApJ, 299, 312
Vicuso, P.J., et al. 1985, ApJ, 296, 149
Watson, D.M., Genzel, R., Townes, C.H., & Storey, J.W.V. 1985, ApJ, 298, 316